Earth Moon Planet (2009) 105:73–80
DOI 10.1007/s11038-009-9313-z

Solar System Observations with MIRI, The Mid InfraRed Instrument on the James Webb Space Telescope

John K. Davies · Gillian S. Wright · Alistair C. H. Glasse

Received: 6 November 2008 / Accepted: 2 May 2009 / Published online: 26 May 2009

Abstract MIRI is the Mid InfraRed Instrument for the James Webb Space Telescope (JWST) and will provide imaging, coronography and integral field spectroscopy in the range between 4.9 and 28.6 μm. We summarise solar system observations which may be possible with this instrument, drawing on examples of observations made with previous space missions such as IRAS, ISO and Spitzer.

Keywords JWST · MIRI · Solar system observations · Comets · Asteroids · Comet trails

1 Introduction

MIRI (Wright et al. 2008) is the Mid InfraRed Instrument for the James Webb Space Telescope (JWST) (Gardner et al. 2006) and will provide imaging, coronography and integral field spectroscopy between 4.9 and 28.6 μm. MIRI operates at the longest wavelengths to be observed by JWST and, unlike the other instruments, is cooled to 7 K by dedicated closed cycle coolers. This is lower than the typical 40 K operating temperature of the rest of JWST. The additional cooling is required for operation of the detectors, and is not intended to reduce the thermal background seen by the instrument which is limited by the telescope itself. Even so, the lower infrared background of the space based JWST compared with ground based telescopes, combined with JWST's much larger aperture than previous infrared space missions, will make MIRI 100–1,000 times more powerful than existing or likely near-future instruments.

The MIRI project is a joint (50–50) European–US development. The European team comprises a very large, nationally funded, consortium of 21 European Institutes from the

Presented at the conference "Future Ground Based Solar System Research, Isola d'Elba, 8–12 September 2008".

J. K. Davies (✉) · G. S. Wright · A. C. H. Glasse
UK Astronomy Technology Centre, Royal Observatory, Blackford Hill, Edinburgh EH9 3HJ, UK
e-mail: jkd@roe.ac.uk

UK, France, Germany, the Netherlands, Switzerland, Belgium, Sweden, Ireland, Denmark and Spain plus contributions from NASA–GSFC and ESA. The main US partner is the NASA Jet Propulsion Laboratory.

2 MIRI Hardware

As shown in Fig. 1 MIRI is divided into three main sections which operate at different temperatures. There is the 40 K optical system which contains the imager and spectrometer pre-optics, the imager and spectrometers themselves and three 1 × 1 k SiAs detectors. One detector is used for imaging and one each in the two arms of the spectrometer. There is an intermediate temperature section which houses interface control electronics and a warm system which includes the closed cycle coolers and their control systems.

The optical system is a lightweighted, homologous, modular system made entirely of aluminium and supported by a thermally isolating carbon fibre hexapod. The imaging and spectroscopy modules are entirely separate, being located on either side of the primary structure. The fields of view of the imager and the spectrometer are defined and separated in the Input Optics and Calibration unit.

The imager includes both a clear area of 75 × 113 arcsec for imaging, and an entrance slit for a low resolution (R ~ 100) spectrometer. There are also four coronagraphs; three quadrant phase masks and one conventional Lyot mask. Each of these four coronographs has its own dedicated filter/pupil mask combination mounted in the filter wheel which lies at a pupil plane. See Table 1 for details of the filters.

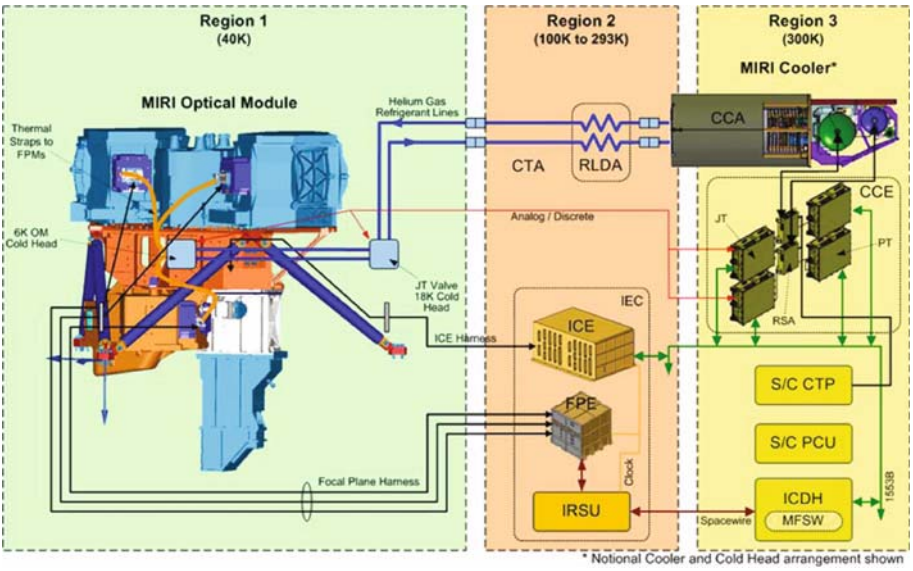

Fig. 1 MIRI system diagram. Subsystems are labelled as follows: *FPM* focal plane module, *JT valve* Joule Thomson valve, *ICE* Instrument Control Electronics (motor and temperature sensor control), *FPE* Focal Plane Electronics (detector control and readout), *CTA* Cooler Tower Assembly, *RLDA* Refrigerant Line Deployment Assembly, *CCA* Cooler Compressor Assembly, *CCE* Cooler Control Electronics, *ICDH* Instrument Control and Data Handling, *MFSW* MIRI Flight Software, *RSA* Relay Switch Assembly

Table 1 MIRI imager/coronograph filters

Name	Imager		Name	Coronograph	
	Wavelength (μm)	Bandwidth (μm)		Wavelength (μm)	Bandwidth (μm)
F560W	5.6	1.2	F1065C	10.65	0.53
F770W	7.7	2.2	F1140C	11.4	0.57
F1000W	10.0	2.0	F1550C	15.5	0.78
F1130W	11.3	0.7	F2300C	23.0	4.6
F1280W	12.8	2.4			
F1500W	15.0	3.0			
F1800W	18.0	3.0			
F2100W	21.0	3.0			
F2550W	25.5	4.0			
F2550WR	25.5	4.0			

Table 2 MIRI medium resolution spectrometer details

Sub-band	Wavelength coverage (μm)	Spectral resolving power ($\lambda/\delta\lambda$)	Pixels per resolution element	
			Spectral	Spatial
1A	4.9–5.8	5,180–6,430	0.9–1.1	1.1–1.7
1B	5.6–6.7	4,800–6,600	0.9–1.2	1.2–1.6
1C	6.5–7.7	4,770–6,480	0.9–1.3	1.2–1.6
2A	7.5–8.8	2,040–5,990	1.1–3.1	1.2–1.7
2B	8.6–10.2	1,770–5,310	1.1–3.7	1.3–1.9
2C	10.0–11.8	1,600–5,000	1.2–4.1	1.5–2.2
3A	11.5–13.6	3,070–5,900	1.0–2.1	1.6–2.0
3B	13.3–15.7	2,390–5,510	1.1–2.2	1.9–2.3
3C	15.3–18.1	2,150–5,040	1.2–2.5	2.2–2.6
4A	17.6–21.0	2,190–2,510	1.7–2.1	2.2–2.7
4B	20.5–24.5	1,950–2,210	1.9–2.4	2.6–4.0
4C	23.9–28.6	1,860–1,950	2.2–2.7	3.1–3.7

The spectrometer comprises two essentially identical arms, each of which contribute to different regions of the 4.9–28.6 μm wavelength coverage. There are four channels, two in each spectrometer module. Complete spectral coverage of each channel is achieved with three grating settings. Details of the wavelength coverage and resolving power are given in Table 2. Note that the imager and spectrometer cover slightly different spectral ranges with the spectrometer coverage extending approximately 1 μm longer than the imager. Each channel of the spectrometer has its own IFU which uses image slicers to deliver extra spatial information over fields of view greater than 3.5 × 3.5 arcsec.

Estimated sensitivities for imaging and spectroscopy are set out in Figs. 2 and 3

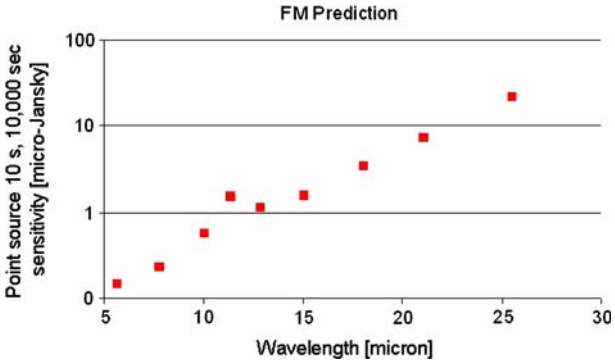

Fig. 2 Predicted MIRI sensitivities for imaging of point sources with continuum spectra, the filter band centres being implicit from the position of the points

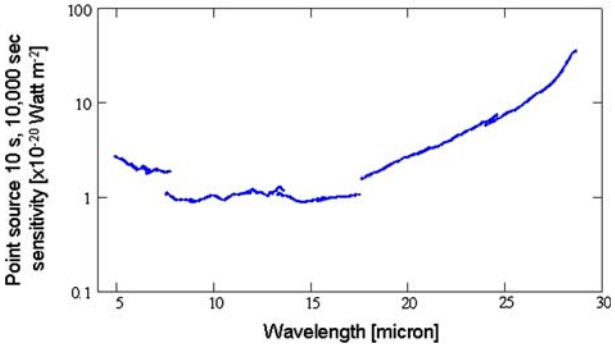

Fig. 3 Predicted MIRI sensitivity for spectroscopy of point sources with narrow (i.e. spectrally unresolved) spectral lines

3 MIRI Observations of Asteroids

Near-IR spectroscopy has been used since the 1970s to determine the surface composition of asteroids from their broad mineral bands in the 0.9–2.5 μm region. The mid-IR has similar promise, but observations are difficult from the ground due to both atmospheric absorptions and the very high background in the 5–25 μm wavelength range. Although spectacular results can be obtained using ground based mid-IR photometry combined with optical observations to determine sizes and albedos of asteroids and comet nuclei (e.g. Müller et al. 2007; Fernandez et al. 2000) ground based mid-IR spectroscopy is very difficult.

Asteroid spectra in this 'thermal' region are dominated by silicate features which include both stretch and bend fundamentals where the interplay between surface and volume scattering create complex emissivity patterns diagnostic of mineralogy, grain size and texture. However, because solar system objects, particularly those in the inner solar system, have significant thermal emission in the MIRI wavelength range, diagnostic spectra can only be determined after a suitable thermal model has been subtracted. In many cases an asteroid Standard Thermal Model (STM) is used to estimate and subtract this thermal flux since more sophisticated models require additional parameters, such as

rotation rate and pole position, which are generally not available. This opens the door to possible pre- and post-mission ground based support to determine these properties for a few high priority or particularly challenging targets.

Space observations with ISO and Spitzer opened a window on this arena of thermal infrared spectroscopy of main belt asteroids. Dotto et al. (2002) used ISO to make low resolution spectra of a small number of main belt asteroids which they compared to meteorite analogues. More recently Spitzer has observed a number of asteroids, for example Barucci et al. (2008) observed 2867 Steins and 21 Lutetia (both secondary targets of the Rosetta mission) and identified spectra consistent with E and C type asteroids.

Emery et al. (2006) have conducted a Spitzer survey of M class asteroids to see if they have mid-IR silicate features which can be correlated with sub-categories of the M class or with physical properties such as radar albedo, near IR mineralogy or 3 μm hydration bands. Emery et al. (2006) present Spitzer data on three Trojan asteroids (1172 Äneas, 911 Agamemnon and 624 Hektor). After removing the thermal background using the STM they were able to analyse the asteroids' spectra in some detail. Their results rule out the presence of organic materials, long suspected to exist on this class of objects, and show that the spectra can be explained purely in terms of silicates. However, the best fit to their data are with observations of silicate dust in the coma of comets. This is not expected in the case of solid surfaces where, unlike in a cometary coma, the individual grains are unlikely to be widely separated. The observations thus provide clues about the surface structure of Trojan asteroids, perhaps suggesting grains suspended in a transparent matrix or 'fairy castle' structures with large numbers of voids. Spitzer will have observed less than two dozen Trojan asteroids before its mission ends, but the extra sensitivity of MIRI will enable a much larger sample of objects to be observed. Interpretation of MIRI data will be greatly assisted by ground based observations to define pole positions etc for improved thermal modelling.

3.1 Comets

Ground based observations have detected 10 μm emission from comets for a number of years, e.g. observations by Hanner and others over many years using the 3.5 m IRTF telescope (see Hanner et al. 1994, 1996 as representatives of many similar papers). These observations, and particularly those of the bright comet C/1995 O1 Hale-Bopp, have shown that typical comet silicates are olivine and pyroxene with Si–O vibrational stretching and bending modes producing the 10 and 20 μm features. Detailed work by, e.g. Wooden et al. (1999), has shown that the fine structure components of these spectra can determine the mineral content (e.g. the Mg:Fe ratio) of these grains and measure how they vary across the coma.

The potential of space observations of comets in the MIRI spectral range was shown by the ISO spectra of C/1995 O1 Hale-Bopp obtained by Crovisier et al. (1997). They determined the spectrum of this comet between 5 and 45 μm and it was soon realised that the comet spectrum was a good match to both IDPs, meteorites and pre-solar system analogues such as the star HD100546. More recently Spitzer spectra of the coma and nucleus of 29P/Schwassmann-Wachmann-1 by Stansberry et al. (2004) has detected features at 9–11 μm (also at 34 μm but these will be outside the MIRI range) and provided a glimpse of what will be possible with MIRI. Spectroscopic observations of C/2001 HT_{50} (LINEAR-NEAT) reported by Kelley et al. (2006) have detected crystalline silicates in a spectrum obtained at 3.2 AU (Fig. 4).

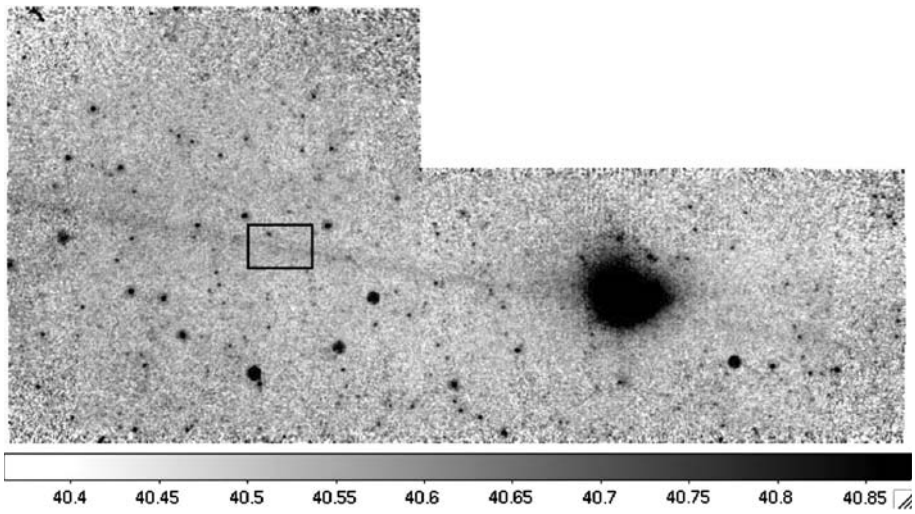

Fig. 4 MIRI imager field of view projected onto Spitzer image of comet 56P/Slaughter-Burnham. This shows that the MIRI field is sufficient to image a reasonable length of trail while retaining some background sky for subtraction. Snapshots along the trail would be required to map the distribution of particle sizes and compositions (*Courtesy*: W. Reach)

Differences in spectra from comet to comet may be the result of different dust properties and/or temperature and MIRI might be expected to observe a number of comets, and to observe some comets repeatedly over a range of heliocentric distances, to make more comparisons possible and resolve this question.

Inactive, ie distant, comets and Centaurs may also make interesting targets, dramatically expanding the SeppCon (http://www.physics.ucf.edu/~yfernandez/seppcon/) programme of Spitzer observations of Jupiter family comets intended to determine effective radii and albedos for a statistically significant number of Jupiter family comets. Although JWST can provide both reflected (near-IR) and emitted (thermal) observations, ground based data to determine lightcurves will be required to fully exploit the JWST data.

3.2 Comet Trails

The existence of meteor streams has long provided evidence that dust is spread around the orbits of periodic comets. Systematic observations of this dust, which can provide information on particle sizes, ejection rates and composition only became possible with the advent of mid-infrared space observatories. The first 'Comet Trail' was detected at 25 μm on comet Tempel-2 using IRAS (Davies et al. 1984) when a series of point like sources detected in near real time at the IRAS preliminary analysis facility were identified as a diffuse structure associated with the comet. The processed IRAS data was explored in detail by Sykes et al. (1986) and Sykes and Walker (1992) who independently identified a number of other such trails. A small number of observations were also made using ISO, for example comet 22P/Kopff (Davies et al. 1997). Several such trails have been observed, and in much more detail, using Spitzer (e.g. Gehrz et al. 2006). The 2P/Encke trail reveals material spread all around the orbit, with particles roughly the size of "sand" grains populating the orbit in R ~ 100 years and larger "gravel" sized particles doing so in R ~ 1,000 years. Using Spitzer, trails have now been detected on numerous comets,

including both known and previously unobserved ones. MIRI can continue and extend this work. Imaging can be used to detect and map fainter trails, searching for any substructure while slit spectra and even spatially resolved spectra using the IFU will be possible.

3.3 Kuiper Belt Objects

The first member of the large population of Kuiper Belt Objects, or trans-Neptunian Objects, was discovered in 1992 (Jewitt and Luu 1993). Since then the trans-Neptunian region has been shown to be very diverse, both in terms of complex orbital structure and compositional properties. However these objects are almost all too distant to be resolved from the ground and so, except for a small number of exceptionally large objects such as 136199 Eris and 90377 Sedna, their sizes and albedos are rather uncertain. This size/albedo degeneracy can be broken if it is possible to obtain simultaneous visible and thermal infrared data, as has been done for many years with the near-Earth and main-Belt asteroids.

MIRI can detect all the known KBOs and together with suitable thermal models this may provide constraints on both the size and albedos of these objects. However the MIRI spectral range only extends to 28.6 μm and this is significantly shortward of the peak emission of these distant, and hence cold, objects, which generally occurs around 80 μm. Observations using the Spitzer long wavelength photometer, which is much better suited to the wavelength range of interest, has already determined albedos for a number of KBO (see the review by Stansberry et al. 2008) and Herschel, which also operates at longer wavelengths than JWST, may well have done many more such observations by the time of the JWST launch. Of course, neither Spitzer nor Herschel will be operational in the JWST timeframe, at which point huge new surveys such as those of Pan-STARRS, the LSST and the GAIA mission may have discovered large numbers of new trans-Neptunians. The more interesting of these may require observations in the thermal-IR that will be impossible without MIRI.

3.4 Status of MIRI in September 2008

In late 2008 the MIRI hardware was coming together well and initial tests on the verification model were encouraging. In terms of image quality VM1 shows flight compatible performance for the F770W, F1130W, F2300C filters and also shows that the instrument transmission is flight-like for these filters. Similarly tests of the spectrometer modules show that the positions of the spectra on the detector and the degree of curvature match the optical models. Background variation as a function of wavelength is also as expected, so there are no indications of major scattered light problems. This is very encouraging and bodes well for the final flight model and the future of MIRI as a powerful tool for solar system astronomy in the next decade.

Acknowledgements John K. Davies thanks to Bill Reach and Josh Emery for their help with the figures and the material on which this talk and paper were based. A number of constructive and helpful comments from the editors greatly improved the original version of this paper.

References

M.A. Barucci, S. Fornasier, E. Dotto, P.L. Lamy, L. Jorda, O. Groussin, J.R. Brucato, J. Carvano, A. Alvarez-Candal, D. Cruikshank, M. Fulchignoni, A&A **477**, 665–670 (2008)

J. Crovisier, K. Leech, D. Bockelee-Morvan, T.Y. Brooke, M.S. Hanner, B. Altieri, H.U. Keller, E. Lellouch, Science **275**, 1904–1907 (1997)
J.K. Davies, S. Green, B. Stewart, A.J. Meadows, H.H. Aumann, Nature **309**, 315–319 (1984)
J.K. Davies, M.V. Sykes, W.T. Reach, F. Boulanger, F. Sibillle, C.J. Cesarsky, Icarus **127**, 251–254 (1997)
E. Dotto, M.A. Barucci, T.G. Müller, J.R. Brucato, M. Fulchignoni, V. Menella, L. Colangeli, A&A **393**, 1065–1072 (2002)
J.P. Emery, L.F. Lim, T. H. McConnochie, Workshop on Early Planetary Differentiation. Sonoma County, CA, LPI Contribution No. 1335, pp. 37–38, 2006
J.P. Emery, D.P. Cruikshank, J. Van Cleve, Icarus **182**, 496–512 (2008)
Y.R. Fernandez, C.M. Lisse, H.U. Kufl, S.B. Peschke, H.A. Weaver, M.F. A'Hearn, P.P. Lamy, T.A. Livengood, T. Kostiuk, Icarus **147**(1), 145–160 (2000)
J.P. Gardner, J.C. Mather, M. Clampin, R. Doyon, M.A. Greenhouse, H.B. Hammel, J.B. Hutchings, P. Jakobsen, S.J. Lilly, K.S. Long, J.I. Lunine, M.J. McCaughrean, M. Mountain, J. Nella, G.H. Rieke, M.J. Rieke, H.-W. Rix, E.P. Smith, G. Sonneborn, M. Stiavelli, H.S.Stockman, R.A. Windhorst, G.S. Wright, Space Sci. Rev. **123**, 485–606 (2006)
R.D. Gehrz, W.T. Reach, C.E. Woodward, M.S. Kelly, Adv. Space Res. **38**, 2031–2038 (2006)
M.S. Hanner, J.A. Hackwell, R.W. Russell, D.K. Lynch, Icarus **112**, 490–495 (1994)
M.S. Hanner, D.K. Lynch, R.W. Russell, J.A. Hackwell, R. Kellogg, D. Blaney, Icarus **124**, 334–351 (1996)
D.C. Jewitt, X.J. Luu, Nature **362**, 730–732 (1993)
M.S. Kelley, C.E. Woodward, D.E. Harker, D.H. Wooden, R.D. Gehrz, H. Campins, M.S. Hanner, S. Lederer, D.J. Osip, J. Pittichova, E. Polomski, ApJ **651**, 1256–1271 (2006)
T.G. Müller, T. Sekiguchi, M. Kaasalainen, M. Abe, S. Hasegawa, in *Near Earth Objects, Our Celestial Neighbors: Opportunity and Risk, Proc IAU Symposium 236*, ed. by G.B. Valsecchi, D. Vokrouhlicky, A. Milani (Cambridge University Press, Cambridge, 2007), pp. 261–266
J.Stansberry, J. Van Cleve, W.T. Reach, D.P. Cruikshank, J.P. Emery, Y.R. Fernandez, V.S. Meadows, K.Y.L Su, K. Misselt, G.H. Rieke, E.T. Young, M.W. Werner, C.W. Engelbracht, K.D. Gordon, D.C. Hines, D.M. Kelly, J.E. Morrison, J. Muzerolle, Astrophys. J. Suppl. **154**, 463–468 (2004)
J. Stansberry, W. Grundy, M. Brown, D.P. Cruikshank, J. Spencer, D. Trilling, J.-L. Margot, in *The Solar System Beyond Neptune*, ed. by M.A. Barucci, H. Boehnhardt, D.P. Cruikshank, A. Morbidelli (University of Arizona Press, Tucson, 2008), pp. 161–180
M.V. Sykes, R. Walker, Icarus **95**, 180–210 (1992)
M.V. Sykes, L.A. Lebosky, D.M. Hunten, F. Low, Science **232**, 1115–1117 (1986)
D.H. Wooden, D.E. Harker, C.E. Woodward, H.M. Butner, C. Koicke, F.C. Witteborn, C.W. McMurray, Astrophys. J. **517**, 1034–1058 (1999)
G. Wright, G. Reike, P. Barella, T. Boeker, L. Colina, E. van Dishoeck, P. Driggers, G. Goodson, T. Greene, A. Heske, T. Henning, P.-O. Lagage, M. Meixner, H. Norgaard-Nielsen, G. Olofsson, T. Ray, M. Ressler, J. Thatcher, C. Waelkens, D. Wright, A. Zehnder, in *Space Telescopes and Instrumentation 2008: Optical, Infrared, and Millimeter*, ed. by J.M. Oschmann Jr., M.W.M. de Graauw, H.A. MacEwen, Proceedings of the SPIE, vol. 7010 (2008)